

# Consistency of the EKF-SLAM Algorithm

Tim Bailey, Juan Nieto, Jose Guivant and Eduardo Nebot

Australian Centre for Field Robotics, University of Sydney  
{tbailey,j.nieto,jguivant,nebot}@acfr.usyd.edu.au

**Abstract.** *This paper presents a simulation-based analysis of the extended Kalman filter formulation of simultaneous localisation and mapping (EKF-SLAM). We show that the algorithm will always produce very inconsistent estimates once the “true” uncertainty in vehicle heading exceeds a limit. This failure is subtle and cannot, in general, be detected without ground-truth, although the inconsistent filter may exhibit observable symptoms, such as “jumpy” vehicle path. Conventional solutions—adding stabilising noise, using iterated or unscented filters, etc—do not improve the situation. However, if “small” heading uncertainty is maintained, EKF-SLAM behaves consistently and is insensitive to system noise and non-linearities. This result indicates the efficacy of submap methods for large-scale maps.*

## 1 Introduction

The original stochastic solution to the SLAM problem by Smith *et al.* [13] is now almost twenty years old, and the concept has reached a state of maturity sufficient to permit practical implementations in challenging environments. Important considerations that have been addressed are reliable data association in cluttered environments [12,1]; reduction of computational complexity through locally partitioned data-fusion [14,6] and conservative data-fusion [6,10,9]; and bounding accumulated non-linearity with submaps [1,3]. However, in spite of its clear success in practical applications, the fundamental consistency of the SLAM algorithm has received little attention.

Non-linear SLAM is predominantly implemented as an extended Kalman filter (EKF), where system noise is presumed Gaussian and non-linear models are linearised to suit the Kalman filter algorithm.<sup>1</sup> EKF-SLAM represents the state uncertainty by an approximate mean and variance. This is a problem in two regards. First, these moments are approximate due to linearisation and may not accurately match the “true” first and second moments. Second, the true probability distribution may be non-Gaussian, so that even the true mean and variance may not be an adequate description. These factors affect how the SLAM probability distribution is projected in time, over a sequence

---

<sup>1</sup> A number of algorithms appearing in the recent literature, such as scan matching [7] and FastSLAM [11], are built on alternative foundations (e.g., data alignment, particle filters), but these have their own problems, both computational and statistical, and are not considered further in this paper. Comparison of EKF-SLAM and FastSLAM will be made in the conference presentation.

of motions and measurements, and how approximation errors accumulate. Previous work on EKF-SLAM consistency [8,4] shows that eventual inconsistency of the algorithm is inevitable for large-scale maps, and the estimated uncertainty will become optimistic when compared to the true errors. While this failure is clearly due to non-linearity, no previous work has examined the root-cause of degeneracy.

In this paper, we show that the fundamental problem with EKF-SLAM is heading uncertainty. This is the single critical factor that causes the map estimate to become inconsistent. All other modelling errors and non-linearities can be adequately compensated with stabilising noise. Inconsistency becomes significant once heading uncertainty is “large enough” and, since heading uncertainty tends to accumulate as the vehicle moves away from the map origin, the problem is inevitable for large maps.

The next section describes the models used in the EKF-SLAM simulation experiments, which are performed in the context of a robot with a range-bearing sensor in a 2-dimensional environment. Data association is assumed known. Section 3 examines the symptoms that manifest once EKF-SLAM becomes inconsistent, and shows that gross inconsistency is entirely due to heading uncertainty. Section 4 discusses the implications of these results and possible solutions to minimise inconsistency, and the final section sums up with concluding remarks.

## 2 Models for EKF-SLAM Experiments

We specify the SLAM state as the vehicle pose (position and heading) and the locations of stationary landmarks observed in the environment. The state at time  $k$  is represented by a joint state-vector  $\mathbf{x}_k$ .

$$\mathbf{x}_k = [x_{v_k}, y_{v_k}, \phi_{v_k}, x_1, y_1, \dots, x_N, y_N]^T = \begin{bmatrix} \mathbf{x}_{v_k} \\ \mathbf{m} \end{bmatrix} \quad (1)$$

Notice that the map parameters  $\mathbf{m} = [x_1, y_1, \dots, x_N, y_N]^T$  do not have a time subscript as they are modelled as stationary.

To describe the vehicle motion, we use the kinematic model for the trajectory of the front wheel of a bicycle subject to rolling motion constraints (i.e., assuming zero wheel slip).

$$\mathbf{x}_{v_k} = \mathbf{f}_v(\mathbf{x}_{v_{k-1}}, \mathbf{u}_k) = \begin{bmatrix} x_{v_{k-1}} + V_k \Delta T \cos(\phi_{v_{k-1}} + \gamma_k) \\ y_{v_{k-1}} + V_k \Delta T \sin(\phi_{v_{k-1}} + \gamma_k) \\ \phi_{v_{k-1}} + \frac{V_k \Delta T}{B} \sin(\gamma_k) \end{bmatrix} \quad (2)$$

Here the time from  $k-1$  to  $k$  is denoted  $\Delta T$ , and during this period the velocity  $V_k$  and steering angle  $\gamma_k$  of the front wheel are assumed constant. Collectively, the velocity and steering values  $\mathbf{u}_k = [V_k, \gamma_k]^T$  are termed the “controls”. The wheelbase between the front and rear axles is  $B$ . The process

model for the joint SLAM state is simply a concatenation of the vehicle motion model and the stationary landmark model.

$$\mathbf{x}_k = \mathbf{f}(\mathbf{x}_{k-1}, \mathbf{u}_k) = \begin{bmatrix} \mathbf{f}_v(\mathbf{x}_{v_{k-1}}, \mathbf{u}_k) \\ \mathbf{m} \end{bmatrix} \quad (3)$$

For a range-bearing measurement from the vehicle to landmark  $\mathbf{m}_i = [x_i, y_i]^T$ , the observation model is given by

$$\mathbf{z}_{i_k} = \mathbf{h}_i(\mathbf{x}_k) = \begin{bmatrix} \sqrt{(x_i - x_{v_k})^2 + (y_i - y_{v_k})^2} \\ \arctan \frac{y_i - y_{v_k}}{x_i - x_{v_k}} - \phi_{v_k} \end{bmatrix} \quad (4)$$

The vehicle motion model, the observation model, and the measured values of the control parameters  $\mathbf{u}_k$ , are not exact, but are subject to noise, which lead to uncertainty in the state estimate. For this reason, we require a probabilistic filter to recursively estimate a distribution over the state given noisy information.

### 3 Problems with EKF-SLAM

The work of Julier and Uhlmann [8] shows that EKF-SLAM inevitably becomes inconsistent and that this problem is structural; it cannot be circumvented by adding stabilising noise to the process and observation models.<sup>2</sup>

We use two measures for filter consistency. When the “true” statistics of the state are available, or can be well approximated, we can compare the true first and second moments ( $\bar{\mathbf{x}}_k, \mathbf{P}_k$ ) with their EKF estimates ( $\hat{\mathbf{x}}_{k|k}, \mathbf{P}_{k|k}$ ). In particular, it is possible to check whether the difference between the true and estimated covariances is positive semi-definite.

$$\mathbf{P}_k - \mathbf{P}_{k|k} \geq \mathbf{0} \quad (5)$$

If it is negative, then the EKF is optimistic. When the true probability density function is not available, but the true state  $\mathbf{x}_k$  is known, we use the *normalised estimation error squared* (NEES) [2, page 234] to characterise the filter performance.

$$\epsilon_k = (\mathbf{x}_k - \hat{\mathbf{x}}_{k|k})^T \mathbf{P}_{k|k}^{-1} (\mathbf{x}_k - \hat{\mathbf{x}}_{k|k}) \quad (6)$$

The consistency of the filter can be found by examination of the average NEES over N Monte Carlo runs of the filter.<sup>3</sup> Under the hypothesis that the

<sup>2</sup> Compensation for inconsistency might be possible by inflating the landmark covariances after each update, but it is not clear how to quantify adequate inflation, and in any case this would nullify all of the SLAM convergence properties described in [5].

<sup>3</sup> A commonly used test of filter consistency is to examine the *sequence* of normalised errors  $\{\epsilon_0, \dots, \epsilon_k\}$  over a *single* run. This test is not adequate as the error sequence is correlated and does not follow a  $\chi^2$  distribution. Thus, even for a linear system, a single run of a consistent filter may appear inconsistent and a single run of an inconsistent filter may appear consistent.

filter is consistent and approximately linear-Gaussian,  $\epsilon_k$  is  $\chi^2$  (chi-square) distributed with  $\dim(\mathbf{x}_k)$  degrees of freedom. Then the average value of  $\epsilon_k$  tends towards the dimension of the state as  $N$  approaches infinity.

$$E[\epsilon_k] = \dim(\mathbf{x}_k) \quad (7)$$

The validity of this hypothesis can be subjected to a  $\chi^2$  acceptance test.

The problem of inconsistency due to large heading uncertainty manifests in two related symptoms. The first is excessive information gain (i.e., reduction in uncertainty), such that the estimated covariance is less than the true covariance. The second is peculiar update characteristics of the state mean, resulting in a jumpy vehicle path and linearly constrained locii of the landmark estimates. The following sections describe these symptoms in detail and present simulation results of the filter consistency under various conditions. In these experiments, the process noise is ( $\sigma_V = 0.3\text{m/s}$ ,  $\sigma_\gamma = 3^\circ$ ) and the observation noise is ( $\sigma_r = 0.1\text{m}$ ,  $\sigma_\theta = 1^\circ$ ), unless otherwise stated. The controls are updated every 0.025 seconds and observations occur every 0.2 seconds.

### 3.1 Symptom 1: Information Gain

To investigate the effect of heading uncertainty on information gain, we first consider a stationary vehicle so that we know throughout the true statistics, and subsequently examine information gain for a moving vehicle.

**Stationary Vehicle** Consider a stationary vehicle with an initial pose estimate

$$\begin{aligned} \hat{\mathbf{x}}_{0|0} &= [0, 0, 0]^T \\ \mathbf{P}_{0|0} &= \text{diag}(\sigma_x^2, \sigma_y^2, \sigma_\phi^2) \end{aligned}$$

The vehicle subsequently observes a single landmark and adds it to the SLAM-map using the feature initialisation procedure described in [1, Section 2.2.4] and [8, Section 2]. Clearly, the true uncertainty of the landmark can never fall below the initial uncertainty of the vehicle pose. Similarly, the true uncertainty of the vehicle pose may never decrease, regardless of how many times the landmark is observed.

For the EKF-SLAM algorithm, the covariance in vehicle position ( $x_v, y_v$ ) does not change. However, the heading variance shows an immediate and dramatic decrease, with the quantity of information gained being dependent on the initial heading variance. The results in Fig. 1 show the spurious information gained for a range of initial heading uncertainties. The quantity of information gained is dependent on the actual observation errors, and so varies from run to run. In Fig. 1, each line represents the worst-case run of 50 Monte Carlo simulations. Notice that the larger initial uncertainties tend to produce the smallest final uncertainty estimates.

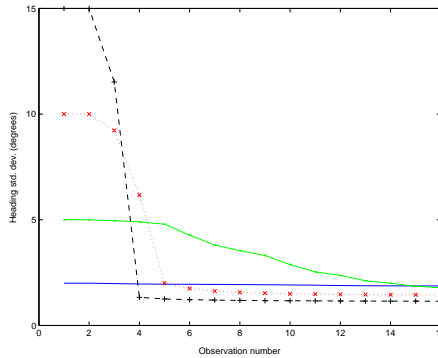


**Fig. 1.** Information gain in heading for a stationary vehicle. This figure shows estimated heading standard deviation  $\sigma_\phi$  after each observation update.

The gain of information for a stationary vehicle is entirely due to the variation in the observation Jacobian  $\frac{\partial \mathbf{h}}{\partial \mathbf{x}_k}$  over the observation sequence. If the Jacobian were to remain fixed (e.g., linearised about the true state), there would be no loss in uncertainty. For a normal EKF run, however, the amount of information gain tends to increase with observation uncertainty  $\mathbf{R}_k$  and, more significantly, with the initial heading variance  $\sigma_\phi^2$ . (Note, information gain is independent of vehicle position variance.)

**Moving Vehicle** To examine information gain for EKF-SLAM with a moving vehicle, we compare the results from a nominal run with those obtained using Jacobians linearised about the true state throughout. Experiments in [8] indicate that using “ideal” Jacobians may not ensure true statistics, but our results show they do provide consistent estimates, and the difference between ideal and EKF Jacobian results is a good indicator of nominal EKF performance.

Fig. 2 shows the result of the two runs. Notice that the covariance estimates of the standard EKF are smaller than for the EKF with ideal Jacobians. This indicates a significant level of information gain in the standard algorithm.<sup>4</sup> The information gain in heading is shown in Fig. 3, where the top line is the ideal Jacobian estimate and the lower line is the standard EKF estimate. This result corroborates with the findings of Castellanos *et al.* [4]. The heading uncertainty for the ideal Jacobian solution grows while ever the vehicle travels further into unmapped territory but, for the standard EKF solution, the heading uncertainty reaches a ceiling and levels off. Here, the

<sup>4</sup> It is interesting to observe in Fig. 2 that the standard EKF estimate appears to be more accurate than the ideal Jacobian estimate. This is purely coincidence, and the standard algorithm is, in fact, inconsistent, but this becomes apparent only by running additional Monte Carlo simulations with the same noise characteristics.

information gain is negligible for heading standard deviation below about 1.7 degrees, but rapidly becomes significant at around 2 degrees.

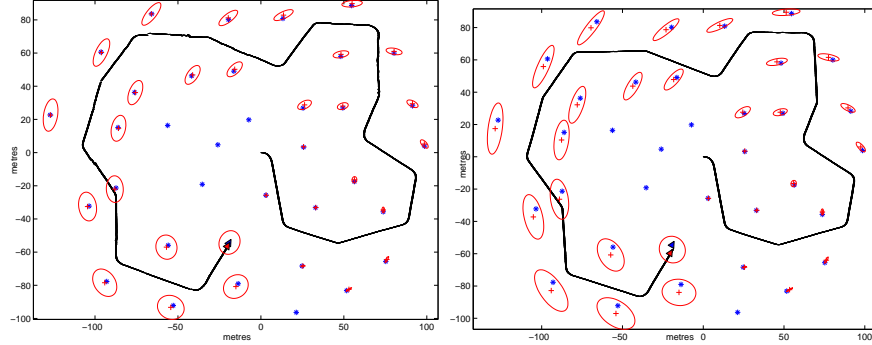


**Fig. 2.** EKF-SLAM simulations showing the estimated vehicle trajectory and 2-sigma ellipses of landmark locations. The true landmarks are shown as stars. The left-hand figure is normal EKF and the right-hand figure is EKF with Jacobians linearised about the true state.

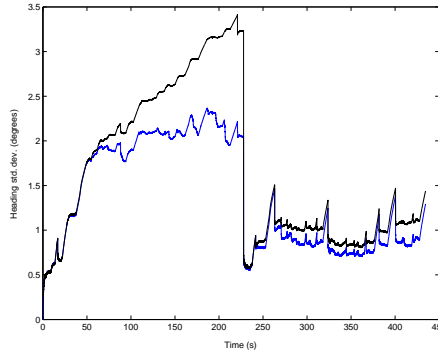


**Fig. 3.** EKF-SLAM heading uncertainty. The vehicle performs *two* loops of the trajectory shown in Fig. 2. The large decrease in uncertainty at 220 seconds is when the vehicle first closes the loop.

If the standard EKF-SLAM algorithm is run with direct observation of the heading at regular intervals, so that the heading uncertainty is always small, the estimated covariance is virtually identical to the ideal Jacobian result. That is, the information gain for EKF-SLAM with small heading uncertainty is negligible. This property is insensitive to the values of process and observation noise.

### 3.2 Symptom 2: Jumpy Path and Constrained Feature Loci

The inconsistency of the EKF-SLAM algorithm becomes visibly evident with the appearance of discontinuities in the estimated vehicle trajectory. Over successive observation updates, the mean estimate of the vehicle pose shows dramatic jumps, which tend to be disproportionately large when compared to the size of the actual measurement error. A related symptom appears in the locii of landmark location estimates. Rather than exhibiting motion in accord with the sensor noise, the landmark mean updates seem to be constrained to a line. Again, the size of the update tends to be much larger than the actual measurement error. These symptoms manifest once the vehicle heading uncertainty becomes “large”, but do not appear if the Jacobians are linearised about the true state (see Fig. 4).

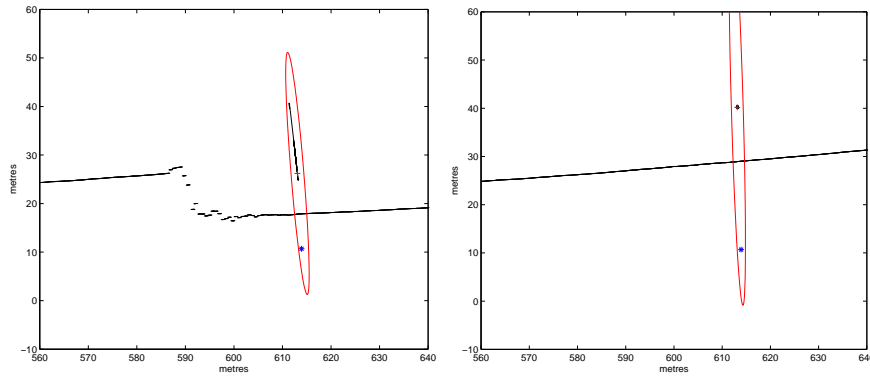


**Fig. 4.** Jumpy path and linear feature locus. The left-hand figure shows a section of the estimated vehicle path and a landmark locus for EKF-SLAM. The right-hand figure shows the estimates given ideal Jacobians.

It is difficult to say precisely why these symptoms appear. The information gain in heading induces over-strong correlations between the vehicle and the landmarks. It would seem that these invalid cross-correlations constrain the feature updates to follow linear paths. Measurements that attempt to shift a landmark estimate orthogonal to a certain line result in large updates *along* the line and large jumps in vehicle pose to compensate.

### 3.3 Monte Carlo Tests of Filter Consistency

Consistency of the EKF is evaluated by performing multiple Monte Carlo runs and computing the average NEES. Given  $N$  runs, the average NEES is computed as

$$\bar{\epsilon}_k = \frac{1}{N} \sum_{i=1}^N \epsilon_{i_k} \quad (8)$$

Given the hypothesis of a consistent linear-Gaussian filter,  $N\bar{\epsilon}_k$  has a  $\chi^2$  density with  $N \dim(\mathbf{x}_k)$  degrees of freedom [2, pages 234–235]. Thus, for the 3-dimensional vehicle pose, with  $N = 50$ , the 95% *probability concentration region* for  $\bar{\epsilon}_k$  is bounded by the interval  $[2.36, 3.72]$ . If  $\bar{\epsilon}_k$  rises significantly higher than the upper bound, the filter is optimistic, if it tends below the lower bound, the filter is conservative.

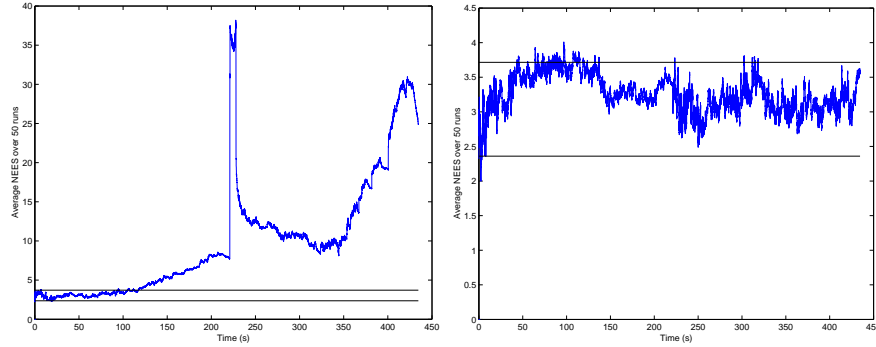


**Fig. 5.** Average NEES of the vehicle pose states over 50 Monte Carlo runs. The left-hand figure is nominal EKF-SLAM and the right-hand figure is with ideal Jacobians.

Fig. 5 shows the average NEES of the vehicle pose states for nominal EKF-SLAM and for the ideal Jacobian case over two loops of the trajectory shown in Fig. 2. The EKF is clearly inconsistent, rising above the upper bound midway through the first loop (at about 120 seconds). There is a large spike at about 220 seconds on closing the loop. The EKF with ideal Jacobians behaves consistently throughout. This shows that the ideal Jacobian simulation, while still a linear filter, is a reasonable estimator of the *true* first and second moments of the state.

The failure of EKF-SLAM is unavoidable; no amount of added stabilising noise improves the result in Fig. 5. However, running the nominal EKF with regular observations of heading, so that the true heading uncertainty is always small, produces consistent results. This result is insensitive to the system noises. For example, we performed experiments with process noise ( $\sigma_V = 1.0\text{m/s}$ ,  $\sigma_\gamma = 5^\circ$ ) and observation noise ( $\sigma_r = 1.0\text{m}$ ,  $\sigma_\theta = 10^\circ$ ), and obtained estimates within the upper/lower NEES bounds, similar to the second plot in Fig. 5. Very long-term runs under these conditions continue to give consistent estimates; SLAM does not fail with time.

## 4 Discussion

Many of the arguments against the EKF-SLAM algorithm do not address the real problem. For example, two common arguments claim it is inadequate



because (i) it poorly linearises the process and observation models, and (ii) it cannot consistently “close the loop”. To investigate (i), we implemented two variants of the EKF: the iterated EKF (IEKF) and the unscented Kalman filter (UKF). Both of these gave similar results to standard EKF-SLAM, indicating that improved local linearisation does not help.<sup>5</sup> With regard to (ii), the failure to properly close large loops tends to occur only if the SLAM estimate is *already* inconsistent due to heading uncertainty. If the state is consistent prior to closing the loop, then the EKF will usually produce a consistent update even when the loop error is large.

Significant improvements in consistency are likely for EKF-SLAM variants that minimise heading uncertainty and minimise variations in Jacobian linearisation. The *constrained local submap filter* (CLSF) [14] is one such method as it performs most updates in a local frame with small heading uncertainty. Batch update methods, such as fixed-interval smoothing between timesteps  $k$  and  $k + N$ , are also likely to help. For very large-scale maps, submap methods, such as *network coupled feature maps* (NCFM) [1] and ATLAS [3], are currently the only solution that avoids data-fusion with large heading variance. Submap methods confine all updates to small-scale maps and use summation over a topology to compute consistent global estimates without information gain.

## 5 Conclusion

In this paper, we have shown that EKF-SLAM *always* fails once true heading uncertainty rises above a limit (typically about 1 to 2 degrees). Inflating the process and observation noise models does not help. Failure is subtle and difficult to detect without ground-truth. The estimated uncertainty simply plateaus while the “true” uncertainty continues to grow. An observable symptom that may occur is a “jumpy” vehicle path, where the vehicle pose update is significantly greater than would be expected from the actual measurement error.

Inconsistency can be prevented if (i) the Jacobians are always linearised about the true state, or (ii) the vehicle heading uncertainty is always small. In either case, the filter is robust to process/observation noises and non-linearities, and minor modelling errors can be adequately compensated with stabilising noise, if necessary. SLAM is stable in the long-term under these conditions.

The IEKF and UKF cannot prevent inconsistency. They offer no significant improvement over plain EKF-SLAM. Batch update methods are likely to extend the region over which EKF-SLAM can construct a consistent global map as they reduce local heading uncertainty and Jacobian variation. For

---

<sup>5</sup> In fact, the IEKF tends to promote divergence as the SLAM state is not locally observable. The IEKF does, however, improve results when closing the loop.

large-scale maps, submaps confine EKF updates to the small-scale, and prevent any data fusion with large heading uncertainty. Submaps are currently the only way to implement large-scale EKF-SLAM without spurious information gain.

## References

1. T. Bailey. *Mobile Robot Localisation and Mapping in Extensive Outdoor Environments*. PhD thesis, University of Sydney, Australian Centre for Field Robotics, 2002.
2. Y. Bar-Shalom, X.R. Li, and T. Kirubarajan. *Estimation with Applications to Tracking and Navigation*. John Wiley and Sons, 2001.
3. M. Bosse, P. Newman, J. Leonard, M. Soika, W. Feiten, and S. Teller. An Atlas framework for scalable mapping. In *IEEE International Conference on Robotics and Automation*, pages 1899–1906, 2003.
4. J.A. Castellanos, J. Neira, and J.D. Tardós. Limits to the consistency of EKF-based SLAM. In *IFAC Symposium on Intelligent Autonomous Vehicles*, 2004.
5. M.W.M.G. Dissanayake, P. Newman, S. Clark, H.F. Durrant-Whyte, and M. Csorba. A solution to the simultaneous localization and map building (SLAM) problem. *IEEE Transactions on Robotics and Automation*, 17(3):229–241, 2001.
6. J. Guivant and E. Nebot. Improving computational and memory requirements of simultaneous localization and map building algorithms. In *IEEE International Conference on Robotics and Automation*, pages 2731–2736, 2002.
7. J.S. Gutmann and K. Konolige. Incremental mapping of large cyclic environments. In *IEEE International Symposium on Computational Intelligence in Robotics and Automation*, pages 318–325, 1999.
8. S.J. Julier and J.K. Uhlmann. A counter example to the theory of simultaneous localization and map building. In *IEEE International Conference on Robotics and Automation*, pages 4238–4243, 2001.
9. S.J. Julier and J.K. Uhlmann. Using multiple slam algorithms. In *IEEE/RSJ International Conference on Intelligent Robots and Systems*, pages 200–205, 2003.
10. J. Leonard and P. Newman. Consistent, convergent, and constant-time SLAM. Technical report, Massachusetts Institute of Technology, Department of Ocean Engineering, 2003.
11. M. Montemerlo, S. Thrun, D. Koller, and B. Wegbreit. FastSLAM 2.0: An improved particle filtering algorithm for simultaneous localization and mapping that provably converges. In *International Joint Conference on Artificial Intelligence*, pages 1151–1156, 2003.
12. J. Neira, J.D. Tardós, and J.A. Castellanos. Linear time vehicle relocation in SLAM. Technical report, University of Zaragoza, Department of Computer Science and Systems Engineering, 2002.
13. R. Smith, M. Self, and P. Cheeseman. A stochastic map for uncertain spatial relationships. In *International Symposium of Robotics Research*, pages 467–474, 1987.
14. S.B. Williams. *Efficient Solutions to Autonomous Mapping and Navigation Problems*. PhD thesis, University of Sydney, Australian Centre for Field Robotics, 2001.